ROYAL SOCIETY
OF CHEMISTRY

PAPER

Check for updates

Post-synthetic fluorination of Scholl-coupled microporous polymers for increased CO$_2$ uptake and selectivity†

Ammar H. Alahmed,[ab] Michael E. Briggs, [ID] [ab] Andrew I. Cooper [ID] *[ab] and Dave J. Adams [ID] *[c]

We report a facile, one-step post-synthetic fluorination method to increase the CO$_2$ capacity and CO$_2$/N$_2$ selectivity of porous organic Scholl-coupled polymers. All of the fluorinated polymers that we synthesised showed increases in CO$_2$/N$_2$ IAST selectivity and CO$_2$ isosteric heat; almost all materials also showed an increase in absolute CO$_2$ uptake. Our best-performing material (SC-TPB F) demonstrated a CO$_2$ capacity and CO$_2$/N$_2$ selectivity of 3.0 mmol g^{-1} and 26 : 1, respectively, at 298 K—much higher than the corresponding non-fluorinated polymer, SC-TPB. This methodology might also be applicable to other polymer classes, such as polymers of intrinsic microporosity, thus providing a more general route to improvements in CO$_2$ capacity and selectivity.

Introduction

Carbon dioxide (CO$_2$) capture and storage from fixed point emission sources is one strategy for reducing CO$_2$ emissions and, hence, the rate of global warming.[1] The current state-of-the-art technology uses aqueous amine solutions to chemically strip CO$_2$ from flue gas streams.[1,2] However, the costly nature of regenerating the amine solutions, their negative environmental impact, and their corrosive nature limit their use on a large scale.[3,4] Recently, physisorptive porous solids have surfaced as promising candidates to replace aqueous amines.[5–7] Porous network materials can be divided into the two subclasses: amorphous materials and crystalline materials. Crystalline porous materials include metal–organic frameworks (MOFs)[8,9] and covalent organic frameworks (COFs),[10–12] while amorphous porous materials include hypercrosslinked polymers (HCPs),[13–15] conjugated microporous polymers (CMPs)[16–18] and porous aromatic frameworks (PAFs).[19–21] Since cost, scalability, and stability are important factors for the commercial application of porous adsorbents for carbon capture applications, we opted to focus on HCPs, and in particular a sub-class of Scholl-coupled HCPs.[22–24] Scholl-coupled polymers meet several of the necessary criteria for post-combustion CO$_2$

capture from flue gas such as moderate cost, availability of starting materials, scalability, and physicochemical stability. They can also possess good levels of porosity. However, for practical applications, an improvement in working CO$_2$ capacity at higher temperatures coupled with increase in CO$_2$/N$_2$ selectivity would be beneficial.[3,25] Our aim here, therefore, was to explore chemical methods to tune such properties in Scholl-coupled HCPs.

Scholl-coupled HCPs are synthesised from electron-rich aromatic building blocks using a stoichiometric amount of a Lewis acid catalyst, here aluminium chloride (AlCl$_3$). Scholl-coupling differs from the hypercrosslinking approach in that it does not require the use of external cross-linkers such as formaldehyde dimethyl acetal (FDA)[15] or the use of monomers with activated methylene groups,[26] both of which result in the formation of methylene bridges between the aromatic rings.[13–15] Instead, Scholl-coupling primarily affords networks that contain direct aryl–aryl bonds, although the incorporation of methylene bridges between the aromatic rings has also been observed due to reactions with the reaction solvent (dichloromethane, DCM).[23] The use of DCM instead of chloroform as the reaction solvent has been reported to afford networks with up to twice the Brunauer–Emmett–Teller surface area (SA$_{BET}$).[23] Unlike other classes of organic polymers, such as CMPs and subsequent PAFs, Scholl-coupled polymers do not require the use of expensive monomers or transition metal catalysts for their synthesis.[22] The reaction time is also usually short, which is not always the case for benzimidazole- and azo-linked polymers.[27–30] In general, benzimidazole- and azo-linked polymers exhibit high SA$_{BET}$ and good CO$_2$ storage capacities and selectivities due to the presence of CO$_2$-polarising groups. The absence of such functionality in the Scholl-coupled polymers

[a]Department of Chemistry, University of Liverpool, Crown Street, Liverpool, L69 7ZD, UK. E-mail: mebriggs@liverpool.ac.uk

[b]Materials Innovation Factory, University of Liverpool, 51 Oxford Street, Liverpool, L7 3NY, UK

[c]School of Chemistry, College of Science and Engineering, University of Glasgow, Glasgow, G12 8QQ, UK. E-mail: dave.adams@glasgow.ac.uk

This journal is © The Royal Society of Chemistry 2019

J. Mater. Chem. A, 2019, 7, 549–557 | 549

results in lower CO_2/N_2 selectivities, despite their good CO_2 capacities.[31–34] Adsorbent selectivity for CO_2 over N_2 is crucial because N_2 makes up nearly 75% of the flue gas stream compared to ~15% for CO_2.[6] Different strategies have been attempted to increase CO_2/N_2 selectivity by incorporating CO_2-polarizing groups such as amines into polymers.[31] In the case of Scholl-coupling, the sensitivity of some of the electron rich monomers such as pyrrole, thiophene, aniline, and fluoroaniline to $AlCl_3$ or the HCl liberated in the reaction can prevent their polymerisation;[22] indeed, attempts in our laboratory to couple these monomers using standard conditions all failed. Monomers with electron withdrawing groups have been reported previously to hinder the crosslinking reaction in the formation of HCPs.[35–37] A different approach to enhance CO_2/N_2 selectivity is post-synthetic modification. For example, aromatic-containing polymers can be derivatised with sulfonic acid or nitro groups, which can then be reacted further to form ammonium salts[33,38,39] or reduced to form amines, respectively;[40] both strategies can result in improved CO_2 uptake and CO_2/N_2 selectivity.

Seeking a facile new method to increase CO_2 uptake and CO_2/N_2 selectivity, we chose to explore electrophilic fluorination as a route to incorporate CO_2-polarizing groups into a pre-formed porous polymer. To the best of our knowledge, post-synthetic modification of organic polymers such as HCPs and Scholl-coupled polymers via the incorporation of fluorine has not been reported before. 1-Chloromethyl-4-fluoro-1,4-diazoniabicyclo[2.2.2]octane bis(tetrafluoroborate), hereafter referred to as Selectfluor®, has been used previously to fluorinate small molecules in the presence of trifluoromethanesulfonic acid (triflic acid) and DCM.[41] We chose to apply this reagent to the fluorination of a range Scholl-coupled polymers. We then assessed the impact of the presence of fluorine in the polymer gas uptakes, CO_2/N_2 selectivities, and isosteric heats of adsorption for CO_2 and CH_4.

Experimental

Materials and methods

Fluoranthene, triphenylene, and 1,1′-binaphthyl were obtained from TCI chemicals, UK. Anhydrous aluminum chloride was obtained from Alfa-Aesar, UK. All other reagents were ordered from Sigma-Aldrich and used as received.

Synthesis of SC-fluorobenzene. Under a nitrogen atmosphere, anhydrous $AlCl_3$ (3.3 g, 25 mmol) was added to a stirred refluxing solution of fluorobenzene (0.47 mL, 5 mmol) in DCM (30 mL) and the mixture was heated under reflux overnight. The suspension was filtered and washed thoroughly with ethanol and water until the filtrate was clear. The solid was then stirred under reflux in chloroform, methanol, ethanol, tetrahydrofuran, and acetone for 6 hours each. The powder was then collected by filtration and dried for 24 hours at 60 °C under vacuum to afford SC-fluorobenzene (yield = 0.57 g).

General procedure for Scholl-coupled network synthesis. The exact procedure for the synthesis of each polymer can be found in the ESI.† In general, under a nitrogen atmosphere, $AlCl_3$ was added to a refluxing solution of dissolved monomer in DCM and the mixture was heated under reflux overnight with

stirring. The suspension was collected by filtration and washed thoroughly with ethanol and water until the filtrate was clear. The solid was then stirred under reflux in chloroform, methanol, ethanol, tetrahydrofuran, and acetone for 6 hours each. The powder was then collected by filtration and dried for 24 hours at 60 °C under vacuum to produce the Scholl-coupled network.

General procedure for fluorination. In a glove box under a nitrogen atmosphere, Selectfluor® (1.0 g, 2.8 mmol) and a Scholl-coupled polymer (200 mg) were charged to a round bottom flask. The flask was sealed and transferred to a fume-hood where anhydrous DCM (20 mL) was added under a flow of nitrogen. The mixture was stirred for 30 minutes then trifluoromethanesulfonic acid (6 mL) was added dropwise. The reaction mixture was then heated at 40 °C for 5 days. After cooling to ambient temperature, the reaction was poured into ice-water, filtered, and washed thoroughly with 5% sodium hydrogen carbonate solution until the pH of the filtrate was no longer acidic. The filter cake was thoroughly washed with water, DCM, and chloroform. The solid was then Soxhlet extracted with chloroform for 3 days before drying under vacuum overnight at 60 °C to yield the corresponding product. (a) SC-TPB was used to yield SC-TPB F (yield = 172 mg). (b) SC-triptycene was used to yield SC-triptycene F (yield = 174 mg). (c) SC-biphenyl was used to yield SC-biphenyl F (yield = 184 mg). (d) SC-binaphthyl was used to yield SC-binaphthyl F (yield = 340 mg‡). (e) SC-fluoranthene was used to yield SC-fluoranthene F (yield = 392 mg‡). (f) SC-naphthalene was used to yield SC-naphthalene F (yield = 352 mg‡). (g) SC-triphenylene was used to yield SC-triphenylene F (yield = 360 mg‡).

Characterization

Fourier transform infrared (FT-IR). FT-IR spectra for all Scholl-coupled polymers were collected on a Bruker Tensor 27 using KBr disks.

Elemental analysis. CH elemental analysis was carried out using a Thermo FlashEA 1112 Elemental Analyser.

Fluorine content analysis. The analysis of fluorine was performed by Exeter Analytical, UK. All polymers were combusted under oxygen followed by the use of ion selective electrode to determine fluorine content as a wt%.

Solid-state nuclear magnetic resonance (SS-NMR). ^{13}C and ^{19}F SS-NMR of all networks were acquired by the University of Durham, UK.

Gas sorption. Nitrogen adsorption and desorption isotherms of all polymer analogues were collected at 77.3 K using an ASAP2420 volumetric adsorption analyser (Micrometrics Instrument Corporation). The SA_{BET} was calculated in the relative pressure (P/P^0) range 0.05–0.25 and total pore volume (V_{Total}) was calculated at $P/P^0 = ca.$ 0.89–0.99.

The Horvath–Kawazoe method was used to determine the pore size distribution in the low pressure region assuming cylindrical pore geometry.[42] Carbon dioxide, methane, and

---

‡ The fluorination of SC-binaphthyl, SC-fluoranthene, SC-naphthalene, and SC-triphenylene were carried out on twice the scale.

550 | J. Mater. Chem. A, 2019, 7, 549–557

This journal is © The Royal Society of Chemistry 2019

nitrogen isotherms were collected up to a pressure of 1 bar on a Micromeritics ASAP2020 at 298 K for nitrogen, 273 and 298 K for methane, and 298, 318, and 328 K for carbon dioxide. All polymer analogues were degassed at 120 °C for 15 hours under dynamic vacuum (10^{-5} bar) prior to analysis.

Scanning electron microscopy (SEM). A Hitachi S 4800 cold field emission scanning electron microscope (FE SEM) was used to collect high resolution imaging of the polymer morphology. The samples were loaded onto 15 mm Hitachi M4 aluminium stubs. Using an adhesive high purity carbon tab, the prepared HCP analogues were coated with gold nanolayer using an Emitech K550X automated sputter coater (25 mA for 2–3 minutes). Imaging was conducted using a mix of upper and lower secondary electron detectors at a working voltage of 3 kV and a working distance of 8 mm.

Thermogravemetric analysis (TGA). TGA was carried out in platinum pans using a Q5000IR analyser (TA instruments) with an automated vertical overhead thermobalance. The samples were heated at 20 °C min^{-1} to 600 °C under nitrogen followed by switching to air at 600 °C or 1000 °C in the case of SC-fluorobenzene.

Results and discussion

We first prepared a library of relatively cheap and easy-to-synthesize Scholl-coupled organic polymers that possessed moderate to high SA$_{BET}$, pore volume, and CO$_2$ absorption capacity. The polymers were derived from the monomers fluorobenzene, 1,3,5-triphenylbenzene, triptycene, biphenyl, 1,1'-binaphthyl, fluoranthene, naphthalene, and triphenylene. All polymers were characterized using ^{13}C SS-NMR, FT-IR, and TGA. The data supported polymer formation and matched the analysis for the previously reported polymers.[23,24] We also evaluated the porosity of the materials (SA$_{BET}$ and pore volume) using nitrogen adsorption–desorption isotherms at 77.3 K, in addition to collecting CO$_2$, CH$_4$, and N$_2$ isotherms at 298 K for N$_2$, 273 and 298 K for CH$_4$ and 298, 318, or 328 K for CO$_2$. Despite the reasonably high CO$_2$ capacities for these polymers (2–3 mmol g^{-1}) at 298 K and 1 bar, their lack of functionality imparts low isosteric heats at the zero-coverage region (24–27 kJ mol^{-1}) and low CO$_2$/N$_2$ selectivities.[27,43–45]

Aromatic electrophilic fluorination of the polymers with Selectfluor® allowed the incorporation of polar fluorine atoms in the polymer with the aim of enhancing the gas uptake, selectivity, and gas affinity of the polymers without significantly impacting the SA$_{BET}$. The fluorinated polymers were evaluated in a similar manner to the unfunctionalised polymers and, additionally, we used ^{19}F SS-NMR and fluorine content assay to assess the degree of fluorination. A Scholl-coupled polymer was also synthesised directly from fluorobenzene (SC-fluorobenzene) for use as a reference material for the post-synthetically fluorinated Scholl-coupled polymers.

Analysis of SC-fluorobenzene

SC-fluorobenzene was synthesized by the addition of anhydrous AlCl$_3$ to a refluxing solution of fluorobenzene in DCM. ^{13}C SS-NMR showed a major peak at 129.6 ppm and a minor peak 108.9 ppm corresponding to substituted and non-substituted aromatic carbons, respectively. A peak at 159.7 ppm represents the fluorinated aromatic carbons, while the low frequency peaks below 30 ppm correspond to methylene cross-linking bridges from incorporation of the reaction solvent, DCM, into the polymer (Fig. S9, ESI†).[23] ^{19}F SS-NMR confirmed the presence of fluorine in the polymer with broad peak appearing at −117.4 ppm (Fig. S9, ESI†). The C–F vibrational band stretch was also evident in the FT-IR at ~1250 cm^{-1}, while the broad peak at *ca.* 3400 cm^{-1} is likely due to trapped moisture within the network (Fig. S18, ESI†). Using oxygen flask combustion followed by ion selective electrode analysis, the loading of fluorine in SC-fluorobenzene was found to be 9.8%: that is, lower than the idealized theoretical fluorine loading of 17.4% (Tables 1 and S1, ESI†). The discrepancy between the expected and measured fluorine content may be due to the incorporation of methylene bridges into the polymer (major effect), entrapped Al salts, or removal of some of the fluorine atoms during the network formation; for example, the cleavage of fluorine was previously observed in the synthesis of the fluorine-containing triazine framework (F-DCBP CTF-1).[45] The calculated fluorine loading of 9.8% translates to roughly 0.6 fluorine atoms per monomer unit. TGA analysis of SC-fluorobenzene under a nitrogen atmosphere showed a loss of 2.0 wt% when heated up to 150 °C, which might be due to entrapped moisture, catalyst and/or reaction solvent within the network (Fig. S10, ESI†).[31,46]

The SA$_{BET}$ calculated from nitrogen isotherms at 77.3 K was found to be 451 m^2 g^{-1} with a low total pore volume of 0.29 cm^3 g^{-1} (Table 1). The combination of a moderate SA$_{BET}$ and a low pore volume resulted in a moderate CO$_2$ uptake of 1.1 mmol g^{-1} at 1 bar and 298 K. However, the CO$_2$ isosteric heat of adsorption (Q_{st}) for the zero coverage region—calculated using Clausius–Clapeyron equation from three different temperature (298, 318, and 328 K)—was 28.5 kJ mol^{-1} (Fig. 1);[47] that is, similar to sulfonic acid-modified PPN-6, which had a high Q_{st} of 30.4 kJ mol^{-1}.[38] CO$_2$/N$_2$ IAST selectivity was calculated to be 20 : 1 from the single-component isotherms assuming a ratio of 15/85 CO$_2$: N$_2$ at 1 bar and 298 K (Fig. S33, ESI†). We ascribed the high selectivity of CO$_2$ over N$_2$ is mostly to the polarity of the C–F bond, which affords a strong interaction with CO$_2$.[48] Methane uptake at 1 bar and 298 K was found to be 0.35 mmol g^{-1} with a Q_{st} of 26.5 kJ mol^{-1} calculated from measurements at two different temperatures (273 and 298 K) (Fig. 1).

Analysis of Scholl-coupled polymers

Scholl-coupling of the monomers was carried out using previously reported literature procedures (Scheme 1).[23,24] In total, seven Scholl-coupled polymers derived from 1,3,5-triphenylbenzene, triptycene, biphenyl, 1,1'-binaphthyl, fluoranthene, naphthalene, and triphenylene were studied. FT-IR of all the Scholl-coupled polymers shows C=C vibrational stretches in the region of 1500–1600 cm^{-1}. The stretch at ~3050 cm^{-1} can be assigned to C–H of the methylene bridges and the vibrational

Table 1 Gas sorption analysis and fluorine content for all polymeric networks

Polymer	SA_{BET} ($m^2 g^{-1}$)	Total pore volume (micropore volume)[a] ($cm^3 g^{-1}$)	Pore-size distribution maxima[b] (nm)	CO_2 uptake at 0.15 bar (298 K)	CO_2 uptake at 1 bar (298 K)	CH_4 uptake at 1 bar (298 K)	CO_2/N_2 IAST[c]	CO_2/CH_4 IAST[c]	Fluorine wt%
SC-fluorobenzene	451	0.29 (0.19)	1.2–1.9	0.27	1.1	0.35	20 : 1	3 : 1	9.75
SC-TPB	2535	1.48 (1.05)	0.9–1.4	0.45	2.4	0.88	10 : 1	3 : 1	—
SC-TPB F	1446	0.86 (0.66)	0.5–0.8	0.65	3.0	0.81	26 : 1	4 : 1	2.96
SC-triptycene	1760	0.89 (0.72)	0.7–1.5	0.52	2.4	0.84	14 : 1	3 : 1	—
SC-triptycene F	1659	0.85 (0.78)	0.4–0.6	0.58	2.7	0.86	22 : 1	3 : 1	0.72
SC-biphenyl	1842	1.27 (0.74)	1.0–1.5	0.52	2.4	0.91	13 : 1	3 : 1	—
SC-biphenyl F	1169	0.82 (0.53)	1.0–1.5	0.66	2.6	0.73	18 : 1	4 : 1	2.03
SC-binaphthyl	1888	1.11 (0.78)	0.8–1.4	0.58	2.6	0.91	15 : 1	3 : 1	—
SC-binaphthyl F	1632	0.85 (0.67)	0.8–1.4	0.63	2.8	0.90	19 : 1	3 : 1	1.48
SC-fluoranthene	1951	0.97 (0.80)	1.0–1.6	0.67	3.0	1.10	11 : 1	3 : 1	—
SC-fluoranthene F	1835	0.90 (0.75)	1.0–1.6	0.68	3.0	0.99	16 : 1	3 : 1	0.81
SC-naphthalene	1169	0.77 (0.48)	0.8–1.4	0.48	2.0	0.72	17 : 1	3 : 1	—
SC-naphthalene F	810	0.45 (0.33)	0.8–1.4	0.68	2.8	0.92	22 : 1	3 : 1	1.43
SC-triphenylene	1460	1.24 (0.60)	0.9–1.5	0.60	2.5	0.97	15 : 1	3 : 1	—
SC-triphenylene F	1376	0.78 (0.57)	0.7–1.5	0.59	2.6	0.90	16 : 1	3 : 1	1.05

[a] Total pore volume calculated from N_2 adsorption isotherms at 77.3 K (micropore volume calculated using Horvath–Kawazoe method). [b] Pore-size distribution maxima calculated using Horvath–Kawazoe method. [c] CO_2/N_2 and CO_2/CH_4 IAST selectivity was calculated from the single-component isotherms at 298 K assuming a molar ratio of 15/85 CO_2 : N_2 and 50/50 CO_2 : CH_4 at 1 bar and 298 K.

stretches in the region of 2850–3000 cm^{-1} are assigned to aromatic C–Hs. Most polymers show a strong water adsorption peak at ∼3400 cm^{-1} (Fig. S18–S32, ESI†) due to physisorbed water. ^{13}C SS-NMR of SC-TPB, SC-triptycene, SC-biphenyl, SC-binaphthyl, and SC-triphenylene showed one peak corresponding to substituted carbons in the range of 137–141 ppm and a non-substituted carbon peak in the range of 129–132 ppm (Fig. S9, ESI†). However, the ^{13}C SS-NMR for SC-naphthalene and SC-fluoranthene showed only one peak in the aromatic region at 130.7 and 137.3 ppm, respectively (Fig. S9, ESI†). The ^{13}C SS-NMRs for SC-naphthalene and SC-fluoranthene are consistent with the literature.[24] The additional carbon peaks below 40 ppm—observed for all the polymers—correspond to the methylene bridges, which are formed as a consequence of using DCM as a reaction solvent (Fig. S9, ESI†).[23,24] The discrepancies between the measured and calculated CH analysis of the Scholl-coupled polymers (Table S1, ESI†) is likely due to adsorption of atmospheric moisture, incorporation of methylene bridges into the polymer, or entrapped Al salts.

The obtained SA_{BET} and pore volume of all the unfunctionalised Scholl-coupled networks were calculated from nitrogen adsorption–desorption isotherms at 77.3 K. The highest SA_{BET} of 2535 $m^2 g^{-1}$ was observed for SC-TPB, while the lowest SA_{BET} of 1169 $m^2 g^{-1}$ was recorded for SC-naphthalene (Table 1). As for SA_{BET}, the pore volume of SC-TPB was the highest recorded, with a value of 1.48 $cm^3 g^{-1}$, whereas the remaining networks were in the range 0.77 to 1.27 $cm^3 g^{-1}$; the lowest again being SC-naphthalene (Table 1). SC-fluoranthene showed the highest CO_2 uptake of 3.0 mmol g^{-1} at 1 bar and 298 K,[24] while the remaining networks varied from 2.0 to 2.6 mmol g^{-1} with the lowest being SC-naphthalene. As for, SC-fluorobenzene, CO_2/N_2 IAST selectivity was calculated from the single-component isotherms assuming a molar ratio of 15/85 CO_2 : N_2 at 1 bar and 298 K (Fig. S33–S47, ESI†). However, the absence of CO_2

polarizing groups in the unfunctionalised Scholl-coupled polymers resulted in lower CO_2/N_2 selectivity than SC-fluorobenzene (10 : 1–17 : 1), which shows a selectivity of 20 : 1. The combination of a low N_2 uptake and narrow micropores, which favour CO_2 uptake,[40,49] resulted in the highest selectivity of 17 : 1 being observed for SC-naphthalene; SC-TPB showed the lowest selectivity of 10 : 1. The reversibility of the CO_2 isotherms is in keeping with a physisorption mechanism, which is required for this class of materials to compete against amine solvents (Fig. 1).[3] The CO_2 Q_{st} of the networks at the zero-coverage region, calculated form 3 different temperatures (298, 318, and 328 K), ranged from 24 to 27 kJ mol^{-1}. The highest Q_{st} were observed for SC-triphenylene and SC-naphthalene with values of 27 and 26 kJ mol^{-1}, respectively (Fig. 1).

CH_4 uptake at 298 K and 1 bar for the Scholl-coupled polymers was between 0.72 and 1.10 mmol g^{-1}; SC-fluoranthene had the highest uptake and SC-naphthalene the lowest (Table 1). The incorporation of fluorine atoms into the polymer has previously been reported to increase the interaction with methane.[50] The relatively high pore volume exhibited by these polymers has little impact on the methane uptake at 298 K and low pressures as it is only at high pressure that the benefit of a high pore volume on methane uptake is observed.[51,52] While SC-fluorobenzene has a high Q_{st} of 26.5 kJ mol^{-1}, due to the presence of fluorine atoms in the polymer,[50] the unfunctionalised Scholl-coupled networks had Q_{st} for CH_4 below 21 kJ mol^{-1} (Fig. 1).

Analysis of the fluorinated analogues

The lack of CO_2 polarizing groups such as nitrogen within the unfunctionalised Scholl-coupled networks results in a moderate CO_2/N_2 selectivity values.[44] As previously discussed in the case of SC-fluorobenzene, the presence of fluorine in the network
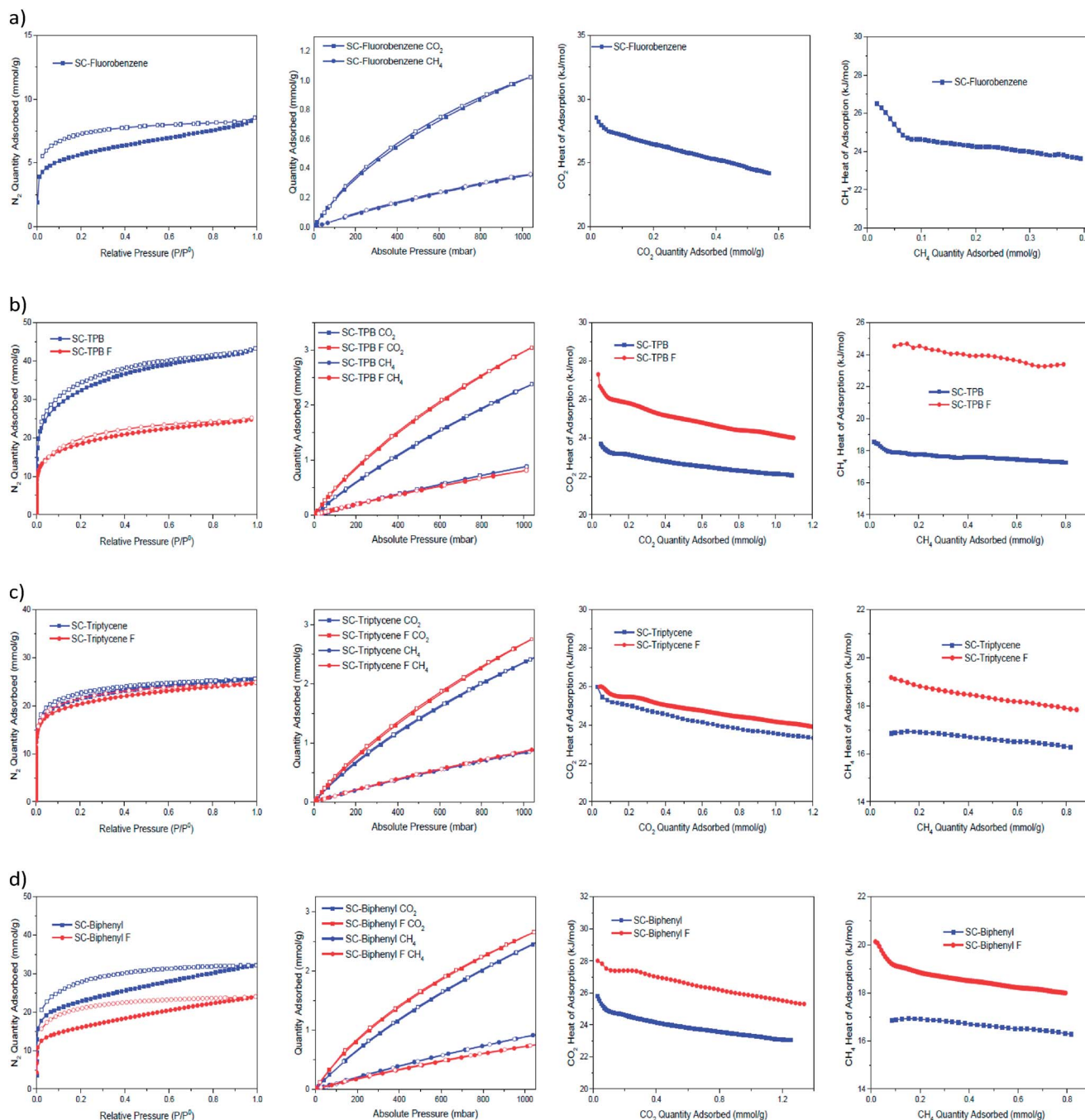
552 | J. Mater. Chem. A, 2019, 7, 549–557

This journal is © The Royal Society of Chemistry 2019

Fig. 1 (Contd.)

afforded enhanced CO_2/N_2 selectivity and Q_{st}, however, it suffers from a moderately low SA_{BET} and pore volume (451 m² g⁻¹ versus for instance 2535 m² g⁻¹ for SC-TPB), which limits is uptake of CO_2 and CH_4. As shown in Table 1, Scholl-coupled polymers with a higher SA_{BET} and pore volume have a higher CO_2 and CH_4 capacity. We therefore chose to introduce polar fluorine atoms into these high surface area polymers by post-synthetic modification. We opted to explore electrophilic fluorination of the Scholl-coupled polymers[53–55] using Selectfluor® and trifluoromethanesulfonic acid (triflic acid) in anhydrous DCM.[41] The proposed mechanism entails the formation of

a protonated trifluoromethanesulfonyl hypofluoride species which then undergoes electrophilic aromatic substitution.[41]

After reaction and purification, the ¹³C SS-NMR of SC-TPB F shows the appearance of a peak at 183.1 ppm, which is consistent with the presence of a carbon–fluorine bond (C–F). This was confirmed by ¹⁹F SS-NMR, which shows a broad peak at −123.0 ppm (Fig. S9, ESI†).[45] The latter was observed in all the fluorinated networks. However, networks that possess non-equivalent aromatic rings in the monomers, such as SC-fluoranthene F and SC-binaphthyl F, also displayed additional peaks, which might correlate to multiple fluorination sites
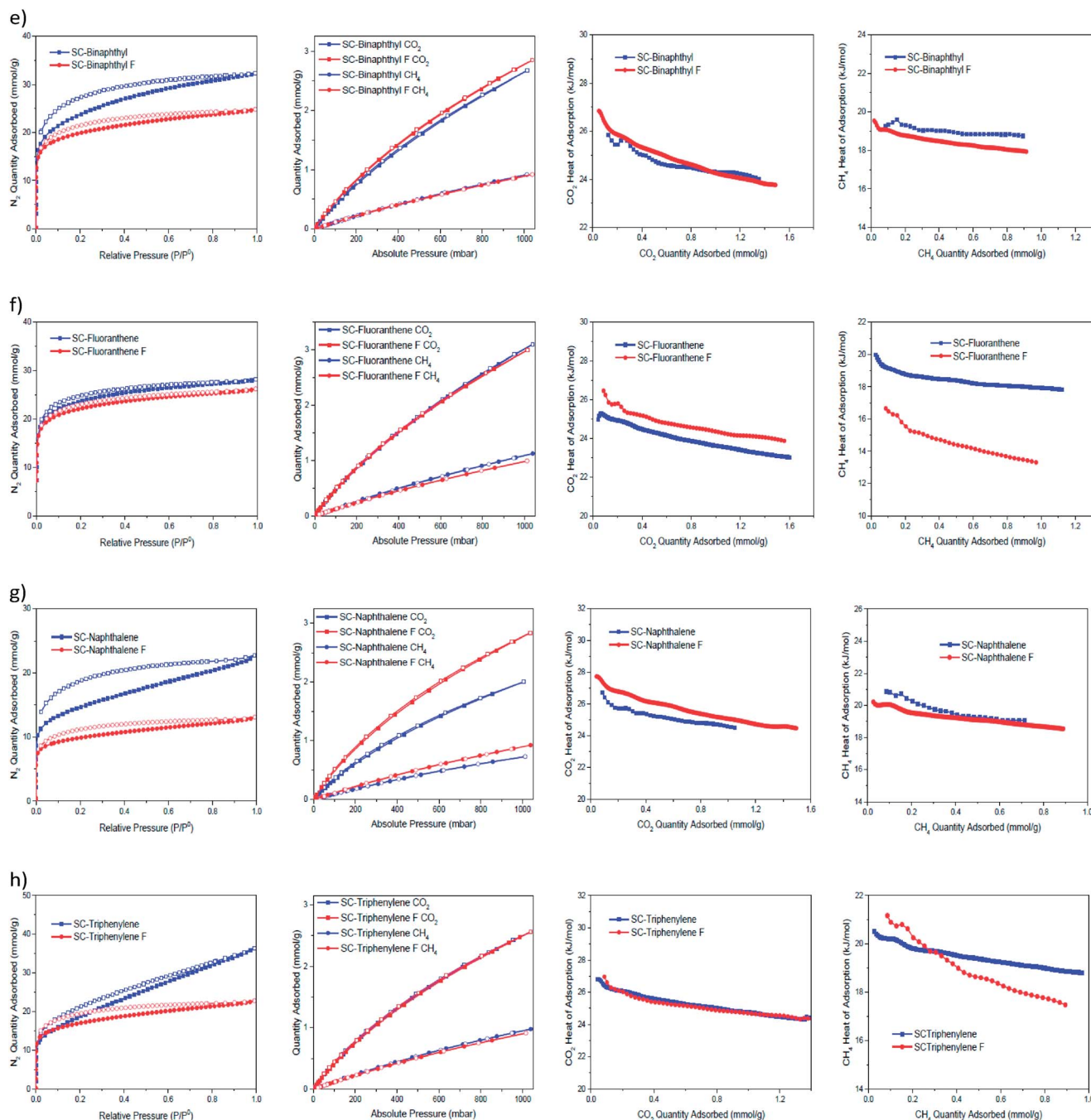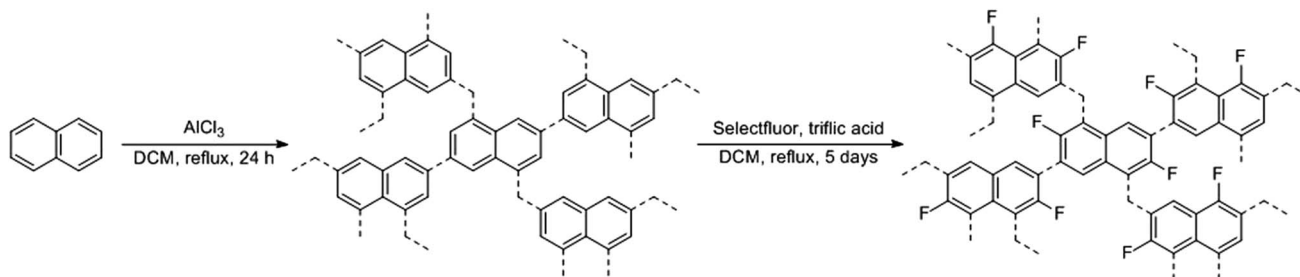
This journal is © The Royal Society of Chemistry 2019

J. Mater. Chem. A, 2019, **7**, 549–557 | 553

Fig. 1 From left to right: N_2 adsorption/desorption isotherms at 77.3 K, CO_2 and CH_4 adsorption/desorption isotherms at 298 K/1 bar, CO_2 isosteric heat of adsorption calculated using Clausius−Clapeyron equation from 3 different temperatures (298, 318, and 328 K) and CH_4 isosteric heat of adsorption calculated using Clausius−Clapeyron equation from 2 different temperatures (273 and 298 K). Closed symbols represent adsorption, open symbols desorption. Blue data points represent the unfunctionalised Scholl-coupled polymers while red data points represent the fluorinated polymers. (a) Represents SC-fluorobenzene; (b) represents SC-TFB; (c) represents SC-triptycene; (d) represents SC-biphenyl. (e) Represents SC-binaphthyl; (f) represents SC-fluoranthene; (g) represents SC-naphthalene; (h) represents SC-triphenylene.

within the polymer (Fig. S9, ESI†).[41,56,57] We also hypothesize that traces of triflic acid and BF_4^- anions from Selectfluor® might be trapped within some of the networks, due to the presence of peaks in the region of −78.5 and −150 ppm, respectively.[58,59] In the case of SC-fluoranthene, SC-triptycene, and SC-triphenylene, the ^{13}C NMR did not show the expected

C–F bond at 182–192 ppm. We attribute this to their low fluorine loading (<1.1 wt%), which might be below the limit of detection for the analysis (Fig. S9, ESI†). The fluorine content in each of the polymers was determined using oxygen flask combustion with ion selective electrode analysis. SC-TFB F was found to have the highest fluorine loading of 2.96 wt%, which

554 | *J. Mater. Chem. A*, 2019, **7**, 549–557

This journal is © The Royal Society of Chemistry 2019

Scheme 1 General reaction scheme, exemplified using naphthalene as the monomer, for the formation of the polymeric networks and the electrophilic fluorination. Naphthalene can be replaced by any of the monomeric units reported in this article.

corresponds to ~0.6 fluorine atoms per monomer (Tables 1 and S1, ESI†). The remaining polymers vary in fluorine content from 0.72 to 2.03 wt%, which corresponds to between 0.1 and 0.3 fluorine atoms per monomer. The relatively low incorporation of fluorine into the polymers could be due to poor accessibility of the reagents to the microporous interior of the polymer, low reactivity of the phenylene units, or a lack of reaction sites due to the presence of multiple Ar–Ar bonds in the polymer. FT-IR of the fluorinated polymers showed the appearance of a peak in the region of 1250 cm^{-1}, which corresponds to the C–F stretch.

In all cases, fluorination of the Scholl-coupled polymers resulted in a decrease in SA_{BET} and pore volume. The biggest decreases were from 2535 m^2 g^{-1} to 1446 m^2 g^{-1} and 1.48 cm^3 g^{-1} to 0.86 cm^3 g^{-1} for SC-TPB F and from 1842 m^2 g^{-1} to 1169 m^2 g^{-1} and 1.27 cm^3 g^{-1} to 0.82 cm^3 g^{-1} for SC-biphenyl F. The decrease in the specific surface area, SA_{BET}, and pore volume correlates with fluorine content and is most likely due to both the larger van der Waals radii of a fluorine atom compared to a proton, and the higher molecular mass of fluorine.

With the exception of SC-fluoranthene and SC-triphenylene F, where almost no change in the CO_2 uptake was observed, fluorination resulted in an increased CO_2 uptake at both 0.15 and 1.0 bar at 298 K for all polymers. SC-TPB F and SC-naphthalene F showed the largest increase in CO_2 uptake of 25 and 40%, respectively, with an increase from 2.4 to 3.0 mmol g^{-1} for SC-TFB F and from 2.0 to 2.8 mmol g^{-1} for SC-naphthalene F, at 1 bar and 298 K. Of greater significance was the increase in CO_2/N_2 selectivity for each of the fluorinated polymers compared with the parent polymers. The biggest increase in CO_2/N_2 selectivity was observed for SC-TPB F where the selectivity more than doubled from 10 : 1 for the parent polymer to 26 : 1. This increase is driven by an increase in CO_2 uptake in at low pressure, due to the more favourable CO_2–polymer interactions caused by the fluorine atoms, and a concomitant decrease in nitrogen uptake.[45,48,60] The CO_2 Q_{st} of SC-TPB F at zero coverage was 27.3 kJ mol^{-1} which represents an increase of 15% compared to SC-TPB (Fig. 1). The same trend of increased CO_2/N_2 selectivity and CO_2 Q_{st} was observed for all fluorine containing polymers, which highlights the positive influence of fluorine incorporation on CO_2-network interactions (Fig. 1). It is clear from these data that post synthetic fluorination gives rise to more promising absorbents for CO_2/N_2 separation than direct coupling of fluorinated monomers.

The presence of fluorine within adsorbents has been reported in the literature to enhance the adsorbent interactions with CH_4, perhaps due to C–F bond polarity.[50] Disappointingly, though, the general pattern of increased CO_2 uptake across the fluorinated analogues was not observed with CH_4. For instance, CH_4 uptake for SC-TPB F—the best performing polymer for CO_2 capture—decreased from 0.88 mmol g^{-1} for the parent polymer to 0.81 mmol g^{-1} at 1 bar and 298 K. SC-naphthalene F was the only polymer in the series that showed an increase in CH_4 uptake from 0.72 to 0.92 mmol g^{-1} at 298 K. Despite the decreased uptake of SC-TPB, its CH_4 Q_{st} was calculated to be 24.5 kJ mol^{-1}, which represents an increase of 32% over SC-TPB. The latter Q_{st} is higher than that of NOTT-108a metal–organic framework (MOF); reported as one of the leading MOFs for methane storage, which possesses a Q_{st} in the zero-coverage region of 16.8 kJ mol^{-1} (calculated from methane isotherms at 273 and 298 K up to 65 bar).[50] SC-fluorobenzene has a higher CH_4 Q_{st} of 26.5 kJ mol^{-1}, but the uptake of CH_4 at 298 K and 1 bar was only 0.35 mmol g^{-1}, less than half that of SC-TPB F. From the remaining polymers, only SC-triptycene F and SC-biphenyl F showed a noteworthy increase of ~2 kJ mol^{-1} to 19.2 and 20.1 kJ mol^{-1}, respectively. It is important to note however, that the full evaluation of the polymers for methane storage would require testing at pressures over 35 bar.[50]

Conclusions

In conclusion, we have successfully incorporated fluorine into a series of microporous Scholl-coupled polymers through post-synthetic modification. Different fluorine loadings were achieved, the highest being observed for the fluorinated network based on TPB (SC-TPB F). A trend of increased CO_2 uptake along with increased CO_2/N_2 selectivity and Q_{st} was observed for all fluorinated Scholl-coupled polymers compared to the unfunctionalised polymers. In the case of our best-performing material (SC-TPB F), CO_2 capacity, CO_2/N_2 selectivity, and CO_2 Q_{st} increased from 2.4 mmol g^{-1}, 10 : 1, and 23.7 kJ mol^{-1} to 3.0 mmol g^{-1}, 26 : 1, and 27.3 kJ mol^{-1}, respectively, at 298 K. The same trend, however, was not achieved for CH_4 with the effect of fluorine atoms on the Q_{st} and CH_4 capacity being inconsistent across the polymer series. However, SC-TPB F has a CH_4 Q_{st} of 24.5 kJ mol^{-1} that rivals that of leading MOFs for methane storage (NOTT-108a).

Conflicts of interest

The authors declare no conflict of interests.

Acknowledgements

Notes and references

1 J. D. Figueroa, T. Fout, S. Plasynski, H. McIlvried and R. D. Srivastava, *Int. J. Greenhouse Gas Control*, 2008, **2**, 9–20.

2 G. T. Rochelle, *Science*, 2009, **325**, 1652–1654.

3 H. A. Patel, J. Byun and C. T. Yavuz, *ChemSusChem*, 2017, **117**, 1515–1563.

4 T. Lewis, M. Faubel, B. Winter and J. C. Hemminger, *Angew. Chem., Int. Ed.*, 2011, **50**, 10178–10181.

5 Y.-S. Bae and R. Q. Snurr, *Angew. Chem., Int. Ed.*, 2011, **50**, 11586–11596.

6 D. M. D'Alessandro, B. Smit and J. R. Long, *Angew. Chem., Int. Ed.*, 2010, **49**, 6058–6082.

7 R. Dawson, A. I. Cooper and D. J. Adams, *Prog. Polym. Sci.*, 2012, **37**, 530–563.

8 M. Eddaoudi, J. Kim, N. Rosi, D. Vodak, J. Wachter, M. O'Keeffe and O. M. Yaghi, *Science*, 2002, **295**, 469–472.

9 K. Sumida, D. L. Rogow, J. A. Mason, T. M. McDonald, E. D. Bloch, Z. R. Herm, T.-H. Bae and J. R. Long, *Chem. Rev.*, 2012, **112**, 724–781.

10 A. P. Côté, A. I. Benin, N. W. Ockwig, M. O'Keeffe, A. J. Matzger and O. M. Yaghi, *Sci. 80*, 2005, **310**, 1166–1170.

11 P. J. Waller, F. Gándara and O. M. Yaghi, *Acc. Chem. Res.*, 2015, **48**, 3053–3063.

12 A. A. Olajire, *J. CO2 Util.*, 2017, **17**, 137–161.

13 V. A. Davankov and M. P. Tsyurupa, *React. Polym.*, 1990, **13**, 27–42.

14 M. P. Tsyurupa and V. A. Davankov, *React. Funct. Polym.*, 2006, **66**, 768–779.

15 B. Li, R. Gong, W. Wang, X. Huang, W. Zhang, H. Li, C. Hu and B. Tan, *Macromolecules*, 2011, **44**, 2410–2414.

16 J.-X. Jiang, F. Su, A. Trewin, C. D. Wood, N. L. Campbell, H. Niu, C. Dickinson, A. Y. Ganin, M. J. Rosseinsky, Y. Z. Khimyak and A. I. Cooper, *Angew. Chem., Int. Ed.*, 2007, **46**, 8574–8578.

17 R. Dawson, A. Laybourn, R. Clowes, Y. Z. Khimyak, D. J. Adams and A. I. Cooper, *Macromolecules*, 2009, **42**, 8809–8816.

18 Y. Xu, S. Jin, H. Xu, A. Nagai and D. Jiang, *Chem. Soc. Rev.*, 2013, **42**, 8012–8031.

19 B. Teng, R. Hao, M. Shengqian, C. Dapeng, L. Jianhui, J. Xiaofei, W. Wenchuan, X. Jun, D. Feng, S. M. Jason, Q. Shilun and Z. Guangshan, *Angew. Chem., Int. Ed.*, 2009, **48**, 9457–9460.

20 W. Lu, J. P. Sculley, D. Yuan, R. Krishna, Z. Wei and H.-C. Zhou, *Angew. Chem., Int. Ed.*, 2012, **51**, 7480–7484.

21 S. Das, P. Heasman, T. Ben and S. Qiu, *Chem. Rev.*, 2017, **117**, 1515–1563.

22 B. Li, Z. Guan, X. Yang, W. D. Wang, W. Wang, I. Hussain, K. Song, B. Tan and T. Li, *J. Mater. Chem. A*, 2014, **2**, 11930–11939.

23 K. J. Msayib and N. B. McKeown, *J. Mater. Chem. A*, 2016, **4**, 10110–10113.

24 S. Hou, S. Wang, X. Long and B. Tan, *RSC Adv.*, 2018, **8**, 10347–10354.

25 T. C. Drage, C. E. Snape, L. A. Stevens, J. Wood, J. Wang, A. I. Cooper, R. Dawson, X. Guo, C. Satterley and R. Irons, *J. Mater. Chem.*, 2012, **22**, 2815–2823.

26 C. D. Wood, B. Tan, A. Trewin, H. Niu, D. Bradshaw, M. J. Rosseinsky, Y. Z. Khimyak, N. L. Campbell, R. Kirk, E. Stöckel and A. I. Cooper, *Chem. Mater.*, 2007, **19**, 2034–2048.

27 A. K. Sekizkardes, S. Altarawneh, Z. Kahveci, T. İslamoğlu and H. M. El-Kaderi, *Macromolecules*, 2014, **47**, 8328–8334.

28 M. G. Rabbani and H. M. El-Kaderi, *Chem. Mater.*, 2012, **24**, 1511–1517.

29 P. Arab, E. Parrish, T. Islamoglu and H. M. El-Kaderi, *J. Mater. Chem. A*, 2015, **3**, 20586–20594.

30 A. K. Sekizkardes, J. T. Culp, T. Islamoglu, A. Marti, D. Hopkinson, C. Myers, H. M. El-Kaderi and H. B. Nulwala, *Chem. Commun.*, 2015, **51**, 13393–13396.

31 R. Dawson, T. Ratvijitvech, M. Corker, A. Laybourn, Y. Z. Khimyak, A. I. Cooper and D. J. Adams, *Polym. Chem.*, 2012, **3**, 2034–2038.

32 H. A. Patel, S. Hyun Je, J. Park, D. P. Chen, Y. Jung, C. T. Yavuz and A. Coskun, *Nat. Commun.*, 2013, **4**, 1357.

33 W. Lu, W. M. Verdegaal, J. Yu, P. B. Balbuena, H.-K. Jeong and H.-C. Zhou, *Energy Environ. Sci.*, 2013, **6**, 3559–3564.

34 C. Gu, D. Liu, W. Huang, J. Liu and R. Yang, *Polym. Chem.*, 2015, **6**, 7410–7417.

35 N. O. Calloway, *Chem. Rev.*, 1935, **17**, 327–392.

36 K. Jiang, D. Kuang, T. Fei and T. Zhang, *Sens. Actuators, B*, 2014, **203**, 752–758.

37 T. Ratvijitvech, M. Barrow, A. I. Cooper and D. J. Adams, *Polym. Chem.*, 2015, **6**, 7280–7285.

38 W. Lu, D. Yuan, J. Sculley, D. Zhao, R. Krishna and H.-C. Zhou, *J. Am. Chem. Soc.*, 2011, **133**, 18126–18129.

39 S. Bhunia, B. Banerjee and A. Bhaumik, *Chem. Commun.*, 2015, **51**, 5020–5023.

40 C. Jian, L. He, Z. Mingmei and Y. Qihua, *Chem.–Asian J.*, 2017, **12**, 2291–2298.

41 T. Shamma, H. Buchholz, G. K. S. Prakash and G. A. Olah, *Isr. J. Chem.*, 1999, **39**, 207–210.

42 G. Horváth and K. Kawazoe, *J. Chem. Eng. Jpn.*, 1983, **16**, 470–475.

43 A. Alabadi, H. A. Abbood, Q. Li, N. Jing and B. Tan, *Sci. Rep.*, 2016, **6**, 38614.

44 Y. He, X. Zhu, Y. Li, C. Peng, J. Hu and H. Liu, *Microporous Mesoporous Mater.*, 2015, **214**, 181–187.

45 G. Wang, K. Leus, H. S. Jena, C. Krishnaraj, S. Zhao, H. Depauw, N. Tahir, Y.-Y. Liu and P. Van Der Voort, *J. Mater. Chem. A*, 2018, **6**, 6370–6375.

46 R. Dawson, E. Stockel, J. R. Holst, D. J. Adams and A. I. Cooper, *Energy Environ. Sci.*, 2011, **4**, 4239–4245.

This journal is © The Royal Society of Chemistry 2019

47 J. A. Dunne, R. Mariwala, M. Rao, S. Sircar, R. J. Gorte and A. L. Myers, *Langmuir*, 1996, **12**, 5888–5895.

48 G. Li, B. Zhang and Z. Wang, *Macromolecules*, 2016, **49**, 2575–2581.

49 L. Tan and B. Tan, *Chem. Soc. Rev.*, 2017, **46**, 3322–3356.

50 G. Chang, H. Wen, B. Li, W. Zhou, H. Wang, K. Alfooty, Z. Bao and B. Chen, *Cryst. Growth Des.*, 2016, **16**, 3395–3399.

51 B. Li, H.-M. Wen, W. Zhou, J. Q. Xu and B. Chen, *Chem*, 2016, **1**, 557–580.

52 W. Hui, S. M. Jason, L. Yun, B. M. Craig, W. Xi-Sen, M. Shengqian, P. K. Vanessa, S. D. Peter, K. J. Cameron, Z. Hong-Cai, Y. Taner and Z. Wei, *Chem.–Eur. J.*, 2010, **16**, 5205–5214.

53 R. P. Singh and J. M. Shreeve, *Acc. Chem. Res.*, 2004, **37**, 31–44.

54 G. I. Borodkin, P. A. Zaikin and V. G. Shubin, *Tetrahedron Lett.*, 2006, **47**, 2639–2642.

55 C. Hollingworth and V. Gouverneur, *Chem. Commun.*, 2012, **48**, 2929–2942.

56 K. Schaumburg, D. Gillies and H. J. Bernstein, *Can. J. Chem.*, 1968, **46**, 503–505.

57 A. Shinji and M. Tohru, *Magn. Reson. Chem.*, 2018, **33**, 639–645.

58 Y. Ao, J. Peng, L. Yuan, Z. Cui, C. Li, J. Li and M. Zhai, *Dalton Trans.*, 2013, **42**, 4299–4305.

59 M. S. Chauhan, G. D. Yadav, F. Hussain and S. Singh, *Catal. Sci. Technol.*, 2014, **4**, 3945–3952.

60 Y. Mizuno, I. Takasu, S. Uchikoga, S. Enomoto, T. Sawabe, A. Amano, A. Wada, T. Sugizaki, J. Yoshida, T. Ono and C. Adachi, *J. Phys. Chem. C*, 2012, **116**, 20681–20687.

This journal is © The Royal Society of Chemistry 2019

J. Mater. Chem. A, 2019, **7**, 549–557 | **557**